PHYSICAL REVIEW C VOLUME 18, NUMBER 5 NOVEMBER 1978

Mesonic and isobar degrees of freedom in the ground state of the nuclear many-body system

M. R. Anastasio, Amand Faessler,* and H. Müther
Institut für Kernphysik der Kernforschungsanlage Jülich, D-5170 Jülich, West Germany

K. Holinde and R. Machleidt†
Institut für Theoretische Kernphysik der Universität Bonn, D-5300 Bonn, West Germany

(Received 5 December 1977)

A study is made in ^{16}O and infinite nuclear matter of the effects of mesonic and isobar degrees of freedom and the effect of the eikonal form factor in the meson-nucleon vertex of the nucleon-nucleon interaction. Three main effects are seen: First, the mesonic degrees of freedom are found to play a significant role by introducing additional density dependence, which results in a large improvement of the radius with a small change in the energy for ^{16}O. Second, when the isobar and mesonic degrees of freedom are combined, repulsion is obtained in ^{16}O with a corresponding increase of the radius. These results are relatively insensitive to the replacement of part of the pionic form factors by the ρ meson in the transition potentials to intermediate states with Δ resonances. Third, the use of the eikonal form factor, instead of phenomenological ones of the dipole type, results in additional attraction. This effect persists when the eikonal form factor is used in a potential that includes mesonic degrees of freedom.

[NUCLEAR STRUCTURE Brueckner-Hartree-Fock in ^{16}O, nuclear matter, mesonic degrees of freedom, one-boson-exchange potential with intermediate isobars.]

I. INTRODUCTION

It is now generally accepted that the nucleon-nucleon (*NN*) interaction is mediated by the exchange of various mesons (see, e.g., Brown and Jackson[1]). However, this fact implies that the standard microscopic procedures for determining the ground state properties of the nuclear many-body system are inconsistent. They start from a phenomenological *NN* potential that is fitted to the two-nucleon scattering data which is then used directly in a Brueckner (for infinite nuclear matter) or Brueckner-Hartree-Fock (for finite nuclei) calculation. By considering a Hilbert space that is composed solely of many nucleon states, the effect of virtual mesons, which couple strongly to the nucleons, has been ignored. In other words, the fact that the nucleon should "feel" the mean field produced by the other nucleons during the meson exchange is not considered.

Several theories have been proposed[2-5] which will account for these extra mesonic degrees of freedom (MDF) and their effects are significant.[6,7] In particular, a density dependence is introduced in the interaction, which leads to different saturation properties in both finite nuclei and infinite nuclear matter than those obtained from standard calculations. This density dependence causes significant changes in this relation in ^{16}O, but not in nuclear matter which is at a higher density.

Another important dynamical feature of the *NN* interaction is the possible excitation of the nucleon, i.e., the isobar degrees of freedom (IDF). The Δ resonance [in particular, the $\Delta(1236)$] can be excited through a meson exchange and then deexcited through a second exchange. Such a process would replace part of the phenomenological σ meson included in one-boson-exchange (OBE) models of the *NN* interaction. Since this excitation is different in the many-body system because of Pauli and dispersion effects, this will also introduce an important density dependence in the interaction which has been studied in the many-body system in Refs. 8–11.

A third feature of the *NN* interaction that has received attention recently[1,12,13] is the replacement of the widely used phenomenological form factors of the dipole type by the eikonal approximation which in free scattering approximates multiple neutral vector meson exchange. This choice depends on s, the square of the invariant energy in the center-of-mass system, and its value is ambiguous in the many-body system. If the view is adopted that the change in the form factor when going from the two-nucleon to the many-body system is kept to a minimum by choosing s as the square of one-half the average kinetic energy, then in the study of the many-body system[14,15] this replacement is found to yield additional binding energy. This is important in view of the repulsion introduced by the isobar degrees of freedom.

In this paper, a study in ^{16}O and nuclear matter is made of the interplay of the effects seen pre-

viously[6,7] from the inclusion of MDF with those from the inclusion of the IDF or of the eikonal form factor. Three different potentials are considered, the first combines the MDF and the eikonal form factor. The other two combine the MDF and IDF, one including the pion only and the second the pion and ρ meson in the transition potentials for the Δ resonance. Some additional effects in the many-body system may be expected when the ρ meson is included. In all the calculations made for ^{16}O in this work, the local density approximation used previously[7,10] is replaced by a direct solution of the Brueckner-Hartree-Fock equations. Details concerning these potentials and their construction are discussed in Sec. II A. In Sec. II B, the methods used to solve the many-body problem in nuclear matter and ^{16}O are discussed. The results of these calculations and a comparison with previous work is made in Sec. III, while some conclusions are presented in Sec. IV.

II. FORMALISM

In this section, the basic ideas involved in the construction of the potentials used to obtain the results given in Sec. III are presented. In addition, the techniques used to determine the ground state properties of ^{16}O and nuclear matter are discussed with particular emphasis on the improved technique used for ^{16}O.

A. Two nucleon system

In this work, calculations using three new nucleon-nucleon (NN) potentials are presented, each of which reproduces the NN-scattering and the two-body bound-state data. All three of these potentials have an energy dependence resulting from the explicit inclusion of mesonic degrees of freedom[1] (MDF). One of them is solely a one-boson-exchange potential (OBEP), while the other two also include explicitly the isobar degrees of freedom (IDF).

The NN-scattering data are obtained for these potentials from a scattering equation of the Lippmann-Schwinger type

$$T(z) = V_{\rm eff}(z) + V_{\rm eff}(z)\frac{P}{z - H_0}\,T(z), \tag{2.1}$$

where z is the starting energy, P is the principal value, and H_0 is the kinetic energy operator. The differences between these three potentials lie in the different definitions of $V_{\rm eff}$.

The OBEP is constructed from a field theoretical Hamiltonian using noncovariant perturbation theory keeping only OBE diagrams. This yields $V_{\rm eff}$ of the form (see Refs. 5 and 15 for details)

$$\langle a'b'|\, V_{\rm eff}(z)|\, ab\rangle = \left\langle a'b' \left| W^{\dagger}\frac{1}{z - \tilde{H}_0}\, W \right| ab \right\rangle_{\rm linked}, \tag{2.2}$$

where W is the field theoretical interaction of the nucleons with the mesons (scalar, pseudoscalar, and vector mesons are considered). Here $\tilde{H}_0$ is the single-particle Hamiltonian, which is just the kinetic energy operator for the NN scattering considered here. These matrix elements of $V_{\rm eff}$ can be obtained from the usual OBEP expressions [Eqs. (2.11)–(2.15) of Ref. 16] by making the substitutions[15]

$$g^2 \to \frac{g^2}{(2\pi)^3}\frac{M^2}{E_q E_{q'}} \quad \text{(and all other coupling constants as well)}, \tag{2.3}$$

$$\frac{1}{(E_q - E_{q'})^2 - (q - q')^2 - \mu^2} \to \frac{1}{\omega_k(z - E_q - E_{q'} - \omega_k)},$$

with $\omega_k = [(q - q')^2 + \mu^2]^{1/2}$. Here μ is the mass of the exchanged meson, M is the nucleon mass, and E_q is the energy of a nucleon with q the momentum in the center-of-mass system.

The OBEP considered here differs from previous work[6,7,15] because of the use of the eikonal form factor[1,12] instead of the more phenomenological ones of the dipole form. In this way, a certain infinite class of higher-order irreducible diagrams are summed approximately. Then $V_{\rm eff}(z) \to V_{\rm eff}(z)F$, where the form factor is given by

$$F = \exp\{2i[\chi(t) - \chi(\mu^2)] + [\chi(u) - \chi(4M^2 - s - \mu^2)]\},$$

$$i\chi(x) = -2\gamma\frac{2M^2 - x}{[x(4M^2 - x)]^{1/2}} \times \arctan\left(\frac{x}{4M^2 - x}\right)^{1/2}, \quad 0 < x < 4M^2 \tag{2.4}$$

$$= -2\gamma\frac{2M^2 - x}{[-x(4M^2 - x)]^{1/2}} \times \ln\left[-\left(\frac{-x}{4M^2}\right)^{1/2} + \left(1 - \frac{x}{4M^2}\right)^{1/2}\right], \quad x < 0.$$

Here s, t, and u are the Mandelstam variables and γ is treated as a parameter. In effect, this OBEP [referred to as MDFPE (mesonic degrees of freedom potential with eikonal form factor)] is constructed using a combination of the approaches of Refs. 13 and 15.

The values of the parameters used in MDFPE are shown in Table I. They yield a good fit to the empirical Livermore analysis[17] of the NN phase shifts as can be seen in Figs. 1 and 2 for the $^1S_0$ and $^3S_1$ partial waves. The resulting low-energy scattering and deuteron data are shown in Table II.

For the potentials which explicitly include the IDF, the form of $V_{\rm eff}$ used in Eq. (2.1) is somewhat different than that given in Eq. (2.2). Instead, $V_{\rm eff}$

TABLE I. Parametrization of the potential MDFPE (mesonic degrees of freedom potential with eikonal form factor). Here values for the coupling constants g^2 and f/g, the meson mass μ and the parameter in the eikonal form factor γ are given for each meson considered.

	g^2	f/g	μ	γ
η	1.0105	0	548.5	1.0
π	14.0	0	138.0	1.0
σ	7.5354	0	564.7	1.0
δ	0.0852	0	960.0	1.0
ω	9.6266	0	782.8	1.0
ρ	0.4738	6.3193	711.0	1.0

now consists of three parts and is given by[18]

$$V_{\text{eff}}(z) = V_{\text{OBE}}(z) + V_{N\Delta}(z)\frac{P}{z-\tilde{H}_0}V_{N\Delta}(z) + V_{\Delta\Delta}(z)\frac{P}{z-\tilde{H}_0}V_{\Delta\Delta}(z)\,. \tag{2.5}$$

It should be noted here that $\tilde{H}_0$ includes the Δ-N mass difference when the Δ resonance is considered explicitly. $V_{\text{OBE}}(z)$ is just the interaction representing OBE [given by Eq. (2.2)], while $V_{N\Delta}(z)$ and $V_{\Delta\Delta}(z)$ are transition potentials that represent the interaction in the $NN \to N\Delta$ and $NN \to \Delta\Delta$ channels, respectively. As in previous work that has included the Δ resonance,[9] the $\Delta\Delta$ vertex, which is poorly known, has been neglected. Equation (2.5) is an extension of the theory given by Schütte[5] in that now the class of diagrams considered in the calculation of many-body processes includes all the linked second-order diagrams as before, plus part of the linked fourth-order graphs, as shown in Fig. 3.

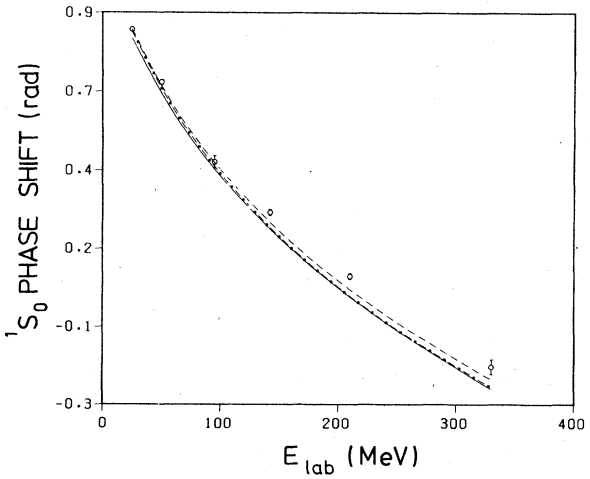

FIG. 1. *NN* nucleon-bar $^1S_0$ phase shifts as a function of the laboratory energy. The error bars are taken from the energy-independent analysis of Ref. 17. Here MDFPE, MDFPΔ1, and MDFPΔ2 are represented by a full, a dashed, and a dot-dashed line and they are mesonic degrees of freedom potentials with eikonal form factor, with $\Delta(\pi)$ and with $\Delta(\pi\rho)$, respectively.

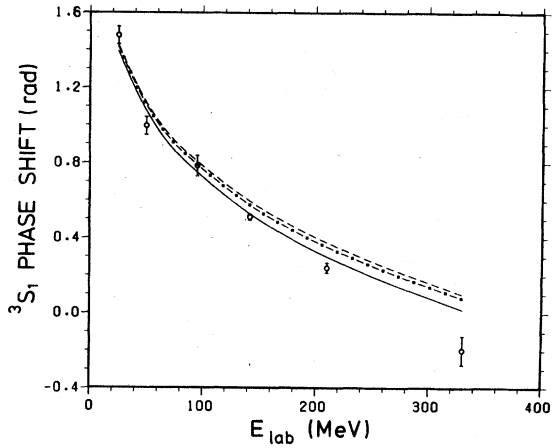

FIG. 2. *NN* nucleon-bar $^3S_1$ phase shifts as a function of the laboratory energy. The notation is the same as in Fig. 1.

In the second potential considered here, only π exchange is included in the transition potentials, as in Ref. 9. The energy dependence in Eq. (2.5) can be introduced into the equation of Ref. 9 as in Eq. (2.3) with the additional prescription that in $V_{N\Delta}$

$$\frac{1}{(q-q')^2+\mu^2} \to \frac{1}{2}\left(\frac{1}{\omega_k(E_q+E_{q'}+\omega_k-z)} + \frac{1}{\omega_k(E_q+E^*_{q'}+\omega_k-z)}\right) \tag{2.6}$$

and in $V_{\Delta\Delta}$

$$\frac{1}{(q-q')^2+\mu^2} \to \frac{1}{\omega_k(E_q+E^*_{q'}+\omega_k-z)}, \tag{2.7}$$

where E^*_q is the kinetic energy of the Δ resonance with momentum q. In contrast to the MDFPE discussed above, this second potential [referred to as MDFPΔ1 (mesonic degrees of freedom potential with $\Delta(\pi)$] does not use the eikonal form factor, rather it follows Ref. 15, i.e., $V_{\text{OBE}} \to V_{\text{OBE}}F_{\text{OBE}}$ with

$$F_{\text{OBE}} = \left(\frac{\Lambda_1^2-\mu^2}{\Lambda_1^2-\Delta^2}\right)^2 \quad \text{for scalar and pseudoscalar mesons,}$$
$$= \left(\frac{\Lambda_2^2-\mu^2}{\Lambda_2^2-\Delta^2}\right)\left(\frac{\Lambda_1^2-\mu^2}{\Lambda_1^2-\Delta^2}\right)^2 \quad \text{for vector mesons,} \tag{2.8}$$

where $\Delta^2 = (E_q - E_{q'})^2 - (q-q')^2$. Similarly, $V_{N\Delta(\Delta\Delta)} \to V_{N\Delta(\Delta\Delta)}F_\Delta$ with

TABLE II. Low-energy scattering and deuteron data. Results are shown for the three potentials MDFPE, MDFP Δ1, and MDFP Δ2 which are mesonic degrees of freedom potentials with eikonal form factor, $\Delta(\pi)$ and $\Delta(\pi\rho)$, respectively. Here E, Q, and P_0 are the binding energy, the quadrupole moment, and the D-state probability of the deuteron, respectively. Also, a_s and a_t are the singlet and triplet scattering lengths while r_s and r_t are the singlet and triplet effective ranges, respectively.

	Experiment	MDFPE	MDFP Δ1	MDFP Δ2
E (MeV)	2.224 62 ± 0.000 06	2.2244	2.2245	2.2249
Q (fm^2)	0.287 5 ± 0.002 0	0.270	0.267	0.280
P_D (%)	5 ± 2	3.1	4.2	4.5
a_s (fm)	-23.715 ± 0.015	-23.72	-23.77	-23.70
r_s (fm)	2.73 ± 0.03	2.66	2.71	2.74
a_t (fm)	5.423 ± 0.005	5.41	5.38	5.40
r_t (fm)	1.748 ± 0.014	1.74	1.69	1.72

$$F_\Delta = \left(\frac{\Lambda^2 - \mu^2}{\Lambda^2 + (q - q')^2}\right)^2 . \tag{2.9}$$

The parameters used in MDFPΔ1 are shown in Table III. A reasonable fit to the phase shifts is obtained, especially at lower energies as seen in Figs. 1 and 2, while the low-scattering and deuteron data are shown in Table II.

The third potential used in this work differs from MDFPΔ1 in that ρ exchange is also included in the transition potentials. The form of $V_{N\Delta}$ and $V_{\Delta\Delta}$ for this potential (referred to as MDFPΔ2 [mesonic degrees of freedom with $\Delta(\pi\rho)$]) is given in Ref. 18. A second minor difference between these two potentials is that now $\Lambda_1 = \Lambda_2$ in Eq. (2.8), i.e.,

$$F_{\rm OBE} = \left(\frac{\Lambda^2 - \mu^2}{\Lambda^2 - \Delta^2}\right)^2 \quad \text{for scalar and pseudoscalar mesons,}$$
$$= \left(\frac{\Lambda^2 - \mu^2}{\Lambda^2 - \Delta^2}\right)^3 \quad \text{for vector mesons} \tag{2.10}$$

instead of the form in Eq. (2.8).

In both MDFPΔ1 and MDFPΔ2 about 20–25% of the intermediate range attraction arises from fourth-order processes [i.e., the second and third terms in Eq. (2.5)]. However, due to the damping effects resulting from the $N\Delta\rho$ vertex, a more reasonable value for the cutoff parameters in the transition potentials is possible for MDFPΔ2, as seen in Table IV. In essence, part of the cutoff effect of the pion form factor in the transition po-

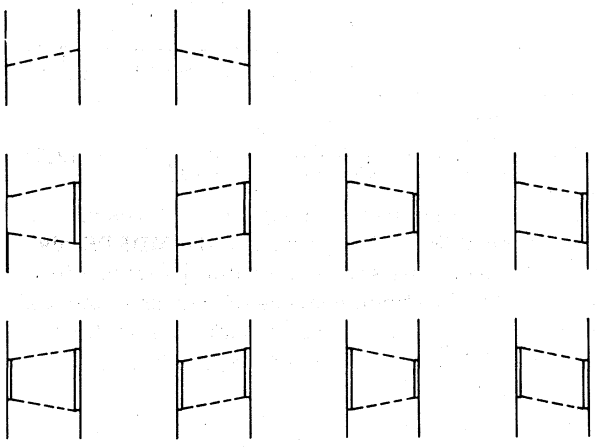

FIG. 3. The second- and fourth-order terms considered in the definition of $V_{\rm eff}$ in Eq. (2.5). Here a solid, a double solid, and a dotted line represent a nucleon, a Δ resonance, and a meson, respectively. Not shown are the exchange graphs and the corresponding set of graphs with the single intermediate Δ resonance on the first line.

TABLE III. Parametrization of the potential MDFP Δ1 [mesonic degrees of freedom potential with $\Delta(\pi)$]. The notation is the same as in Table I except that a distinction must be made between parameters for $V_{\rm OBE}$ and for $V_{N\Delta}$ and $V_{\Delta\Delta}$, referred to as OBE and Δ, respectively. Here Λ_1 and Λ_2 are the cutoff masses in the form factors of Eq. (2.8) for OBE and Eq. (2.9) for Δ. The coupling constants in square brackets are defined by using $[\Lambda_1^2/(\Lambda_1^2 - \Delta^2)]^2$ in Eq. (2.8) instead of $[(\Lambda_1^2 - \mu^2)/(\Lambda_1^2 - \Delta^2)]^2$ and are actually used in the calculations.

	g^2	f/g	μ	Λ_1	Λ_2
OBE: η	9.29 [8.4136]	0	548.5	2500	...
π	13.6 [13.5]	0	138.0	2500	...
σ	7.48 [6.776]	0	548.2	2500	...
δ	1.04 [0.759]	0	960.0	2500	...
ω	24.69 [10.0301]	0	782.8	1300	10 000
ρ	1.81 [0.7794]	3.6495	763.0	1300	10 000
ϕ	28.11 [4.1538]	0	1020.0	1300	10 000
Δ: π	0.36	0	138.0	800	...

TABLE IV. Parametrization of the potential MDFP Δ2 [mesonic degrees of freedom potential with $\Delta(\pi\rho)$]. The notation is the same as in Table III except the cutoff mass Λ now refers to Eq. (2.10) for OBE.

	g^2	f/g	μ	Λ
OBE: η	4.9978	0	548.5	2000
π	14.4	0	138.0	2000
σ	13.5416	0	599.7	1300
δ	0.0718	0	960.0	1300
ω	30.012	0	782.8	1650
ρ	0.4701	6.61	711.0	1650
ϕ	5.3613	0	1020.0	1650
Δ: π	0.27	0	138.0	1200
ρ	15.4	0	711.0	1200

tentials in MDFPΔ1 is replaced by the effects from the $N\Delta\rho$ vertex in the transition potentials in MDFPΔ2.

B. Many-body system

The binding energy of infinite nuclear matter is given in lowest-order Brueckner theory by

$$E=\sum_{i<k_F}\langle i|t|i\rangle+\frac{1}{2}\sum_{i,j<k_F}\langle ij|G(z)|ij\rangle\,, \tag{2.11}$$

where t is the kinetic energy operator, k_F is the Fermi momentum, and z is the starting energy defined as sum of the single-particle energies $z=\epsilon_i+\epsilon_j$. The G matrix is given by

$$G(z)=V_{\rm eff}(z)+V_{\rm eff}(z)\frac{Q}{z-H_0}G(z)\,, \tag{2.12}$$

where Q is the Pauli operator for nucleons. The single-particle energies ϵ_i are determined self-consistently for states below the Fermi surface by the BBP theorem[19]

$$\epsilon_i=t_i+\sum_{j<k_F}\langle ij|G(\epsilon_i+\epsilon_j)|ij\rangle\,,\quad i<k_F \tag{2.13}$$

and $\epsilon_i=t_i$ for states above the Fermi surface. Here t_i is the kinetic energy of the nucleon. This method will differ from the usual procedure because of the form of $V_{\rm eff}(z)$. Here it is given by

$$\begin{aligned}V_{\rm eff}(z)&=V_{\rm OBE}(z)\,,\\&=V_{\rm OBE}(z)+V_{N\Delta}(z)\frac{Q}{z-\tilde{H}_0}V_{N\Delta}(z)\\&\quad+V_{\Delta\Delta}(z)\frac{1}{z-\tilde{H}_0}V_{\Delta\Delta}(z)\,,\end{aligned} \tag{2.14}$$

where the former case holds for MDFPE and the latter for MDFPΔ1 and MDFPΔ2. The mass renormalization corrections arising from the inclusion of mesonic degrees of freedom have been neglected.[6]

The energy dependence of $V_{\rm eff}$ in Eq. (2.14) is expected to give a repulsive effect in nuclear matter.[6] The size of this effect in MDFPE can be tested by comparing the results using Eq. (2.14) (where it should be recalled that $z=\epsilon_i+\epsilon_j$) and

$$V_{\rm eff}=V_{\rm OBE}(t_i+t_j)\,. \tag{2.15}$$

This effect can be tested for potentials with the Δ resonance as well by taking $V_{\rm eff}$ as

$$\begin{aligned}V_{\rm eff}(z)&=V_{\rm OBE}(t_i+t_j)+V_{N\Delta}(t_i+t_j)\frac{Q}{z-\tilde{H}_0}V_{N\Delta}(t_i+t_j)\\&\quad+V_{\Delta\Delta}(t_i+t_j)\frac{1}{z-\tilde{H}_0}V_{\Delta\Delta}(t_i+t_j)\,.\end{aligned} \tag{2.16}$$

Note that here $V_{\rm eff}$ is still energy dependent, but this is not due to the inclusion of mesonic degrees of freedom. This additional energy dependence, along with the inclusion of the Pauli operator Q, is due to the inclusion of the Δ resonance and its effect is also repulsive.[9] Consequently, the two effects are kept separate. The size of the effects due to the Δ resonance can be seen when $V_{\rm eff}$ is given by

$$\begin{aligned}V_{\rm eff}(z)&=V_{\rm OBE}(z)+V_{N\Delta}(z)\frac{1}{t_i+t_j-\tilde{H}_0}V_{N\Delta}(z)\\&\quad+V_{\Delta\Delta}(z)\frac{1}{t_i+t_j-\tilde{H}_0}V_{\Delta\Delta}(z)\,.\end{aligned} \tag{2.17}$$

Finally, all the many-body effects can be "turned off" if $V_{\rm eff}$ is taken as

$$\begin{aligned}V_{\rm eff}&=V_{\rm OBE}(t_i+t_j)+V_{N\Delta}(t_i+t_j)\frac{1}{t_i+t_j-\tilde{H}_0}V_{N\Delta}(t_i+t_j)\\&\quad+V_{\Delta\Delta}(t_i+t_j)\frac{1}{t_i+t_j-\tilde{H}_0}V_{\Delta\Delta}(t_i+t_j)\,.\end{aligned} \tag{2.18}$$

In order to obtain the ground state properties of finite nuclei, the Brueckner-Hartree-Fock (BHF) equations must be solved [the analogous equations for the finite nucleus to Eqs. (2.11)–(2.13)]. This involves an additional self-consistency problem not present for the case of nuclear matter since the single-particle wave functions are not known. The single-particle potential h must be determined and the G matrix must be computed in this basis. In principle, this could be done by solving Eq. (2.12) repeatedly (for each HF iteration), but this would be extremely time consuming computationally. Here a method to solve the BHF equations is used that is tractable computationally and avoids the local density type approximation used in previous work.[7,10,20]

Following the method of Sauer,[21] a reference G matrix $G_{\rm EE}$ is constructed using the Eden-Emery Pauli operator $Q_{\rm EE}$.[22] This reference G matrix is then corrected using an oscillator Pauli operator Q_0, defined in terms of harmonic oscillator

wave functions, where the Q_0 appropriate for ^{16}O is given by

$$Q_0|ab\rangle = \begin{cases} 0 & \text{for } a \text{ or } b = 0s_{1/2}, 0p_{3/2}, \text{ or } 0p_{1/2}, \\ |ab\rangle & \text{otherwise}. \end{cases} \tag{2.19}$$

Then the oscillator G matrix G_0 is

$$G_0(z) = G_{EE}(z) + G_{EE}(z)\left(Q_0 \frac{1}{z - H_0} Q_0 - Q_{EE} \frac{1}{z - H_0} Q_{EE}\right) G_0(z). \tag{2.20}$$

This equation is solved using matrix inversion including single-particle states up to $2n + l = 9$ ($n = 0, 1, \ldots$). Finally, the self-consistent G matrix would be obtained by correcting for the difference between the self-consistent Q and Q_0 with an equation similar to Eq. (2.20). If this equation is iterated then

$$G(z) = G_0(z) + G_0(z)\left(Q \frac{1}{z - H_0} Q - Q_0 \frac{1}{z - H_0} Q_0\right) G_0(z) + \cdots. \tag{2.21}$$

The convergence of this series has been checked[23,24] and found to be very rapid, especially for ^{16}O. Consequently, only the first term in Eq. (2.21) is retained here, which should be sufficient since relative effects are the main concern here. For the rearrangement terms in which the dependence on the density plays the important role, the first two terms are included [see Eq. (2.23)].

So far, the single-particle operator has not been defined. For the solution of the G matrix equation, this must be specified only for the particle states. Here it is taken as a pure kinetic energy plus a constant shift. However, because the potentials considered here are all energy dependent then the hole state energies must also be specified to define $\bar{H}_0$ in Eqs. (2.2) and (2.5). In order to solve Eq. (2.20), the single-particle energies are parametrized as

$$\epsilon_k = \begin{cases} k^2/2M - C, & k > k_F, \\ k^2/2M^* - A - C, & k < k_F. \end{cases} \tag{2.22}$$

Of course, M^* and A must be adjusted to reproduce the self-consistent energies after the HF iterations have been performed. Fortunately, the final results are not very sensitive to their values.[7]

In addition to the usual BHF choice for the self-consistent single-particle potential, two rearrangement terms are considered as well. The inclusion of these additional terms amounts to the Landau definition[25] of the single-particle potential as the functional derivative of the energy with respect to the density, if the energy is considered in the HF approximation. Then

$$h = \frac{\partial \langle H \rangle}{\partial \rho} = h^{BHF} + \left\langle \frac{\partial G}{\partial z} \frac{\partial z}{\partial \rho} \right\rangle + \left\langle \frac{\partial G}{\partial Q} \frac{\partial Q}{\partial \rho} \right\rangle. \tag{2.23}$$

The consideration of the first term alone will be referred to as BHF, the first two terms as renormalized BHF (RBHF) and all three terms as density dependent HF (DHF).

III. RESULTS

The purpose of this work is to test the effects in the many-body system of different forms of the NN interaction which all fit the two-nucleon data reasonably well, allowing a meaningful nuclear structure calculation. Traditionally, such a calculation would be made in infinite nuclear matter, instead of in finite nuclei, because of the relative difficulty of the calculations. However, the standard Bethe-Brueckner-Goldstone calculations at nuclear matter density have been questioned recently in light of the results using the Fermi hypernetted-chain method, while this discrepancy is not so large at lower densities. This suggests that one of the light nuclei is a more appropriate system because for its lower density the many-body calculations are more reliable. For this reason, ^{16}O will be considered here. Results from a nuclear matter calculation are also included for completeness and in the hope that valid statements can still be made regarding the relative effects being studied here.

Solving the BHF equations (see Sec. II B) yields the results shown in Figs. 4–6 and Table V. In all cases, the intermediate hole state energies are parametrized using $M^*/M = 0.41$ and $A = 55.8$ MeV in Eq. (2.22), following Ref. 7. Except for the cases indicated in Fig. 6, a pure kinetic energy spectrum is assumed for the intermediate particle energies (i.e., $C = 0$). In Fig. 4, the results of solving the BHF equations using the methods of Sec. II B are compared with those using a local density type approximation for the Pauli operator as in Refs. 7, 10, and 20. This comparison has been made for three potentials, two of which do not include mesonic degrees of freedom (OBEP1[20,26] and HM2[10,13]) and one of which does[7,15] [referred to as MDFP (mesonic degrees of freedom potential) here]. In the former cases, the local density approximation for the Pauli operator underestimates the binding energy while in the latter case it overestimates the binding energy and underestimates the radius.

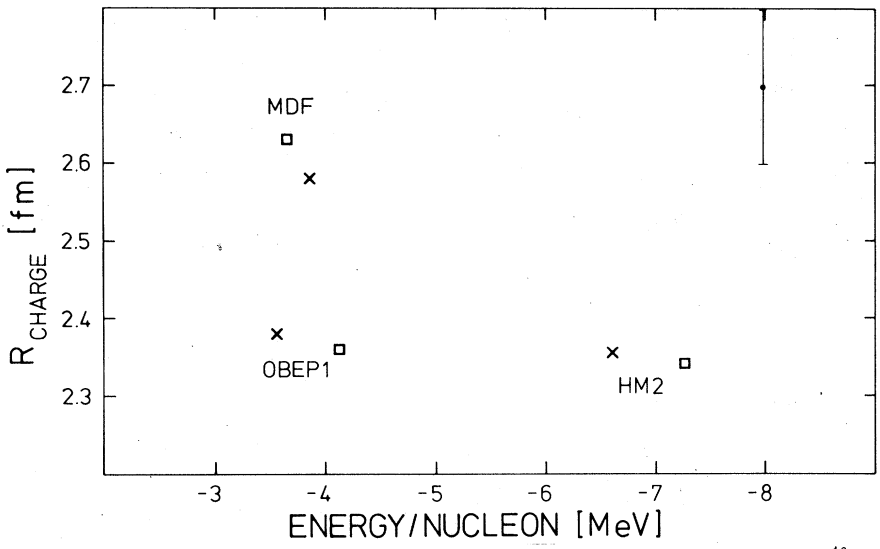

FIG. 4. The total energy per particle as a function of the charge radius for BHF calculations in ^{16}O. The potentials considered are MDFP, which is a mesonic degrees of freedom potential from Ref. 15, and OBEP1 and HM2, which are potentials without and with the eikonal form factor from Refs. 26 and 13, respectively. Here a cross refers to calculations using the local density approximation (Refs. 7, 8, 10, and 20), while a square refers to the method described in Sec. II B.

This can be understood qualitatively. In a local density approximation, the Pauli operator Q_{LD}, in the equation for the G matrix, is approximated by its value in nuclear matter with a larger k_F for OBEP1 and HM2 (which yield a smaller radius) than for MDFP (which yields a larger radius). Now it seems that the Pauli operator for the finite nucleus ^{16}O is less sensitive to the density of the nucleus than Q_{LD}. Consequently, the local density approximation overestimates the Pauli effect for OBEP1 and HM2, leading to a less attractive G matrix and less binding energy, while the approximation underestimates the Pauli effect for MDFP, leading to a more attractive G matrix and a more binding energy.

One final comment should be made at this point regarding the improved calculations with MDFP. Using the old method, Faessler *et al.*[7] noted that

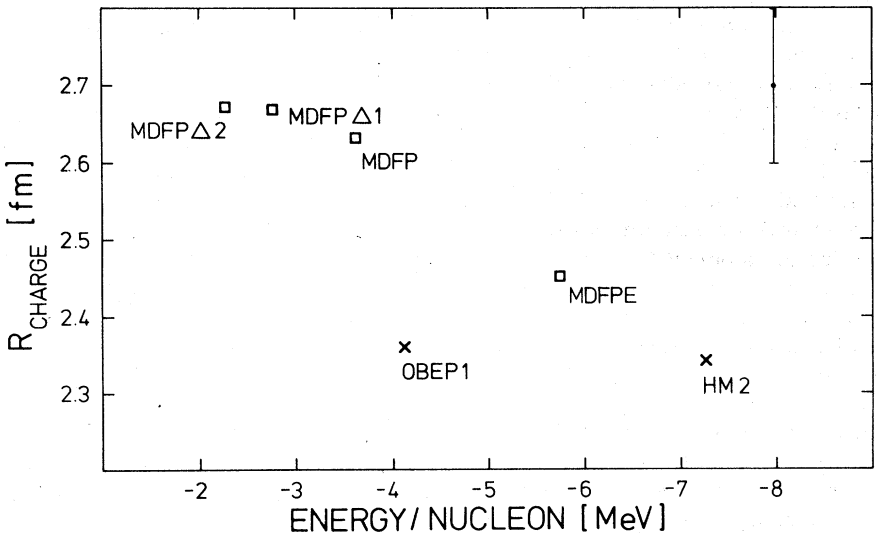

FIG. 5. The total energy per particle as a function of the charge radius for BHF calculations in ^{16}O. The BHF method described in Sec. II B is used for MDFP, MDFPE, MDFP Δ1, and MDFP Δ2 [all mesonic degrees of freedom potentials without eikonal form factor, with eikonal form factor, with $\Delta(\pi)$ and with $\Delta(\pi\rho)$ respectively] and for OBEP1 (Ref. 26) and HM2 (Ref. 15) (without and with eikonal form factor, respectively).

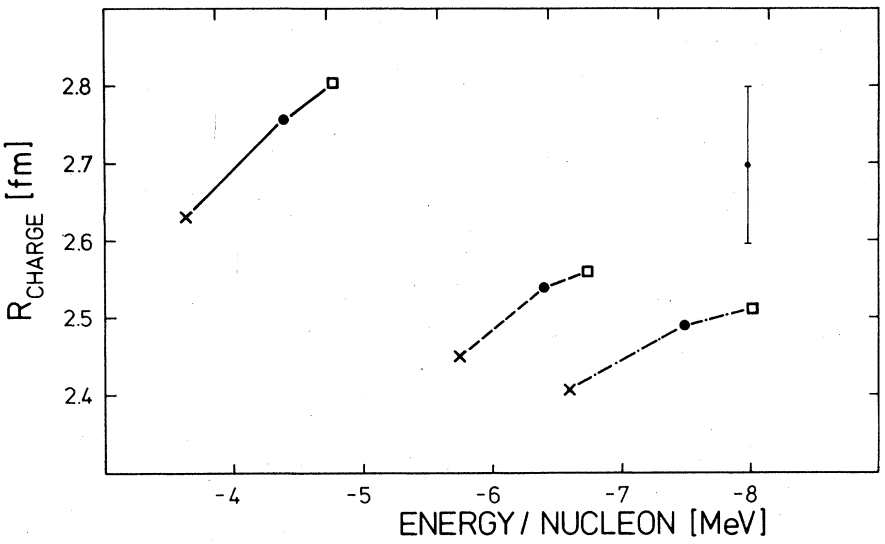

FIG. 6. The total energy per particle as a function of the charge radius for BHF, RBHF, and DHF calculations in ^{16}O represented by a cross, dot, and square, respectively. The solid line refers to MDFP (mesonic degrees of freedom potential) with $C=0$, the dashed line to MDFPE (mesonic degrees of freedom potential with eikonal form factor) with $C=0$ and the dot-dashed line to MDFPE with $C=8$.

a comparison of the binding energy and radius obtained with MDFP and with OBEP1 showed a change that is not expected using standard Brueckner methods and phase-shift equivalent *NN* potentials. They found that the radius using MDFP increases substantially along with a small increase in the binding energy over the results using OBEP1. In Fig. 4 it can be seen that with a more accurate solution of the BHF equations, these results change somewhat, now the large increase in radius when the mesonic effects are included is accompanied by a decrease in the binding energy. However, this decrease is still much smaller than would be expected with phase-shift equivalent potentials. This point will be discussed again below.

In Fig. 5, the results in ^{16}O for the new potentials described in Sec. II A are shown. It should be noted at this point that there is some ambiguity in the use of the eikonal form factor in finite nuclei. This form factor is derived for two-nucleon scattering by summing a certain infinite class of higher-order diagrams, but it is not clear what form this sum will take in a many-body system. However, if it is considered as a phenomenological form (as for the dipole form factor), then the eikonal form factor should be the same in the many-body system as it is in the two-body system. The problem then arises as to how to define the Mandelstam variable s in Eq. (2.4). For scattering it is the square of the energy in the c.m. system of the initial state. But in finite nuclei, the kinetic energy of a single particle is not a good quantum number. In this work, one-half of the oscillator kinetic energy per particle is used for the relative single-particle energy. If instead of the oscillator approximation one-half the kinetic energy per particle resulting from the self-consistent wave function is used, this energy changes from 7.88 to 8.33 MeV for MDFPE (mesonic degrees of freedom potential with eikonal form factor). Then the binding energy per particle increases by about 1% or about 0.06 MeV. However, if double the oscillator value is used, then the binding energy per particle increases by about 2 MeV. On the other hand, if self-consistent single-particle energies are used instead of kinetic energies then the binding energy per particle decreases by about 6 MeV with a large increase in the radius as well. All of this indicates that while the eikonal form factor is an important form for *NN* scattering, its application to finite nuclei is rather ambiguous.

From Fig. 5, it can be seen that the use of an eikonal form factor as in MDFPE instead of a dipole form factor as in MDFP results in substantially more binding energy. Thus this feature, seen previously by Holinde *et al.*,[10] persists when the mesonic effects are also included. But the results from both MDFP and MDFPE relative to those from OBEP1 and HM2, respectively, are different from the results expected for phase-shift equivalent potentials. As discussed in Ref. 7 regarding MDFP, this effect arises from the starting energy dependence of MDFP because of the explicit inclusion of mesonic degrees of freedom. The self-consistent single-particle energies must

be used in MDFP and MDFPE, which makes the energy denominator in Eq. (2.2) larger in magnitude thereby reducing the magnitude of $V_{\text{eff}}(z)$, especially for deeply bound states. This will lead to a less attractive G matrix and, consequently, the absolute value of the single-particle energies decreases. On the other hand, this starting-energy dependence introduces an additional density dependence in the G matrix. This leads to a larger radius and smaller kinetic energy, which partly compensates the decrease in potential energy. A small decrease in the binding energy and large increase in radius results as seen in Fig. 5.

However, the increase in radius due to the inclusion of mesonic degrees of freedom (MDF), as seen in Fig. 5, is smaller when HM2 and MDFPE (both OBE potentials using the eikonal form factor) are compared. There is a larger change in binding energy and smaller change in radius than in the MDFP vs OBEP1 case. This can be understood from the increased attraction and more deeply bound single-particle states (see Table V) when the eikonal instead of the dipole form factor is used. This means that the G matrix (and consequently the potential) is evaluated at a more negative starting energy for which the derivative $\partial G/\partial z$ is smaller. Consequently, the density dependence of the effective interaction via a change of the starting energy is reduced. Therefore the additional influence of the density dependence introduced by the inclusion of MDF, which is also a density dependence due to a change of the starting energy, is reduced. This then leads to a smaller change in the radius and kinetic energy. However, since the propagator in $V_{\text{eff}}(z)$ gets smaller with the use of more bound single-particle energies from MDFPE, the potential energy will be reduced in magnitude even more than above resulting in a larger change in binding energy. The change of the propagator is important in second order in V_{eff} only. However, the second order terms are less important relative to the Born term, as reflected in the smaller D-state probability in the deuteron, for MDFPE thereby partly reducing the effects from the propagator.

The repulsion due to the explicit inclusion of isobar degrees of freedom (IDF) shown by Holinde *et al.*[10] also persists when the mesonic effects are included, as seen from the results of MDFPΔ1 [mesonic degrees of freedom potential with $\Delta(\pi)$] and MDFPΔ2 [mesonic degrees of freedom potential with $\Delta(\pi\rho)$] in Fig. 5. It is interesting to note that the shift in the binding energy relative to MDFP seen here (1.1 and 1.4 MeV) is similar to the corresponding shift of HM2 + Δ(450) relative to HM2 (0.9 MeV[10]) and that in all three potentials MDFPΔ1, MDFPΔ2, and HM2 + Δ(450), approximately 20–25% of the σ meson has been replaced by the isobar.

TABLE V. The self-consistent BHF calculations in ^{16}O for various NN potentials. The potentials considered [MDFP (Ref. 15) MDFPE, MDFP Δ1, and MDFP Δ2) are all mesonic degrees of freedom potentials without eikonal form factor, with eikonal form factor, with $\Delta(\pi)$, and with $\Delta(\pi\rho)$, respectively. The single-particle energies ϵ are given for proton states along with the total energy per nucleon (E/A) and the radius of the charge distribution (R_{ch}) corrected for center-of-mass motion.

	MDFPE	MDFP	MDFP Δ1	MDFP Δ2
ϵ: $\pi 0s_{1/2}$ (MeV)	-47.79	-36.11	-32.86	-31.74
ϵ: $\pi 0p_{1/2}$ (MeV)	-21.70	-16.35	-14.56	-13.64
ϵ: $\pi 0p_{3/2}$ (MeV)	-18.90	-14.41	-12.72	-11.60
E/A (MeV)	-5.75	-3.69	-2.76	-2.28
R_{ch} (fm)	2.45	2.63	2.67	2.67

As noted in Sec. II A, the addition of the $N\rho$ vertex in MDFPΔ2 allows a weaker cutoff in the form factor for the transition potentials than in MDFPΔ1. In effect, part of the pion form factor, which was chosen to be independent of the many-body dynamics, in MDFPΔ1 has been replaced by the $N\Delta\rho$ vertex, which introduces many-body effects because of the ρ-meson propagator. Some differences between these two potentials might then be expected in the results for the many-body system, although these differences should be small due to the short range of the $N\Delta\rho$ vertex. From Fig. 5, MDFPΔ2 yields a smaller radius relative to MDFPΔ1 than would be expected from comparing saturation properties of phase shift equivalent potentials. However, this difference is small enough that it could be attributed to uncertainties in the calculations, in particular, differences in the fits of these two potentials to the NN data, so that no definite conclusion can be drawn here regarding the effects of the $N\Delta\rho$ vertex.

In Fig. 6, results for MDFP and MDFPE are shown for different choices of the HF procedure used, i.e., HBF, RBHF, and DHF as discussed in Sec. II B. It should be noted that the change from BHF to RBHF is larger for MDFP than for MDFPE. Since the additional term entering RBHF is proportional to $\partial G/\partial z$ [see Eq. (2.23)] this supports the view taken above that there is less sensitivity to the density dependence arising from the starting energy for MDFPE.

The results for a second value of the shift parameter C in the particle spectrum [see Eq. (2.22)] are also given for MDFPE. The choice of $C = 8$ MeV originates from the work of Zabolitzky,[27] who showed for the Reid soft-core potential that the

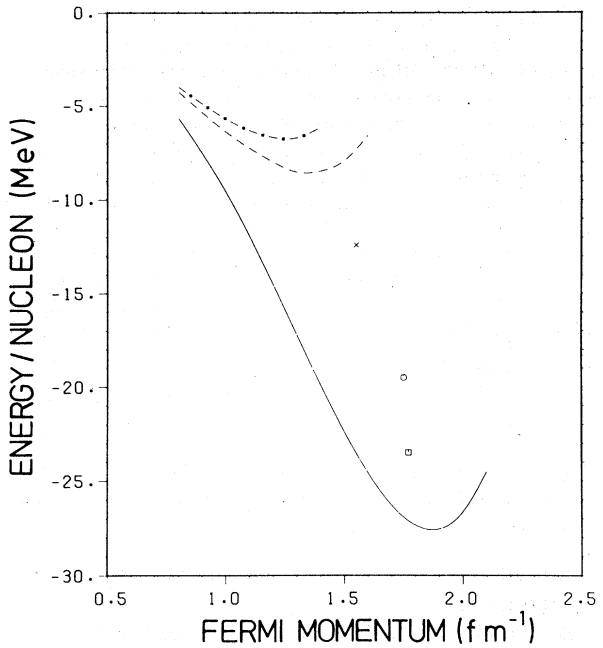

FIG. 7. The total energy per particle as a function of the Fermi momentum k_F for nuclear matter. The full, dashed and dot-dashed lines represent the results for MDFPE, MDFP $\Delta 1$, and MDFP $\Delta 2$ [mesonic degrees of freedom potentials with eikonal form factor, with $\Delta(\pi)$ and with $\Delta(\pi\rho)$, respectively]. The saturation points for OBEP1 (Ref. 26), MDFP (Ref. 6), and HM2 (Ref. 14) represented by a cross, a circle, and a square, respectively, are given as well.

effects of three-body clusters can be minimized for finite nuclei like ^{16}O for this choice. It is made here as well so that comparison with previous work can be made, but rigorously it can no longer be justified in terms of minimizing higher-order terms since the propagator in the potential as well as in the G matrix is dependent on C.

The trends seen here for these additional calculations, where a second choice of C and different choices of the HF procedure are used, are the same as in previous work again confirming the independence of these effects on the inclusion of MDF. These same additional calculations have been made for MDFPΔ1 and MDFPΔ2, although they are not shown, and quite similar results are obtained.

The results for the calculations in infinite nuclear matter are shown in Fig. 7 and Tables VI–VIII. As mentioned at the beginning of this section, the standard Brueckner calculations at nuclear matter densities have been questioned. Consequently, relative effects only will be discussed here. A comparison of similar potentials with and without mesonic degrees of freedom, e.g., MDFPE vs HM2 or MDFP vs OBEP1, shows different effects in nuclear matter (see Fig. 7) than in ^{16}O. Here MDFPE (or MDFP) yields more binding energy at a larger density than HM2 (or OBEP1), while in ^{16}O it yields less binding energy at a smaller density. As discussed previously, the MDF introduce density dependence into the potential and that this causes the effects seen in ^{16}O. Since nuclear matter is a denser system than ^{16}O, differences in this effect can be expected. In addition, in ^{16}O changes in the binding energy can show up through a change in the self-consistent wave functions and a resulting change in the kinetic energy, which is not possible in nuclear matter. There the changes in binding energy seem to be related to differing D-state probabilities of the deuteron for the potentials.[6]

Also in Fig. 7, it can be seen that the use of the eikonal instead of the dipole form factor (MDFPE vs MDFP) yields substantially more binding energy, as found previously,[6] even when the mesonic effects are included. Again this is related to the D-state probabilities (3.2% vs 4.4%, respectively). Also the inclusion of IDF (MDFPΔ1 or MDFPΔ2 vs MDFP) results in repulsion, as previously,[9] when mesonic effects are included as well. More repulsion, almost 2 MeV at saturation, is obtained when the ρ meson is included in the transition potentials. This could be due to effects arising from the replacement of part of the pion form factor by the $N\Delta\rho$ vertex, as mentioned regarding ^{16}O. However, this result could be explained if a larger amount of the intermediate range attraction has been replaced by the IDF when the ρ meson is included. The precise amount is difficult to determine from the phase shifts since the effects are nonlinear, but some statements regarding this are made below. The fits to the NN data are not equivalent either which also causes some uncertainty so that the $N\Delta\rho$ effects cannot be isolated.

An explicit way of seeing the effects in the many-body system from the IDF would be to "turn off" these effects. As discussed in Sec. II B, this can be done by using Eq. (2.17) instead of Eq. (2.14) to define V_{eff}. The results are shown in Tables VI and VII, in the second column labeled "no effects in Δ," for each partial wave with $k_F = 1.4$ fm^{-1}. This is done using the same self-consistent single-particle potential obtained from the "full" interaction (these results are shown in the first column) so that the results can be compared. That the inclusion of the isobars should lead to a repulsive effect is clear since the second and third terms in Eq. (2.14) are attractive but many-body effects reduce it: Both the presence of the Pauli operator and the dispersion effect from the use of the self-consistent single-particle energies to define the starting energy reduce the magnitude of

TABLE VI. Partial wave contribution in MeV to the binding energy of nuclear matter for MDFP Δ1 [mesonic degrees of freedom potential with $\Delta(\pi)$] at $k_F = 1.4$ fm^{-1}, with and without many-body effects. Here the results of the self-consistent calculation defining V_{eff} by Eq. (2.14) are shown in the first column. "No Δ effects," "no mesonic effects," and "no many-body effects" refer to a non-self-consistent calculation defining V_{eff} by Eq. (2.17), Eq. (2.16), and Eq. (2.18), respectively.

	MDFP Δ1	MDFP Δ1 No Δ effects Eq. (2.17)	MDFP Δ1 No mesonic effects Eq. (2.16)	MDFP Δ1 No many-body effects Eq. (2.18)
$^1S_0$	-14.02	-15.35	-16.51	-20.32
$^3P_0$	-3.76	-3.84	-3.88	-4.00
$^1P_1$	3.29	3.27	3.27	3.22
$^3P_1$	12.76	12.19	11.82	10.89
$^3S_1$	-20.39	-20.83	-23.02	-24.59
$^3D_1$	1.55	1.55	1.55	1.55
$^1D_2$	-2.53	-2.66	-2.73	-2.91
$^3D_2$	-4.32	-4.32	-4.34	-4.35
$^3P_2$	-6.24	-6.76	-7.18	-8.30
$^3F_2$	-0.60	-0.50	-0.47	-0.39
$J = 3$	2.99	2.97	2.93	2.89
$J = 4$	-1.70	-1.71	-1.72	-1.74
$5 \leqslant J \leqslant 12$	0.49	0.49	0.49	0.49
Total potential E	-32.48	-35.49	-39.80	-47.56
Kinetic E	24.02	24.02	24.02	24.02
E	-8.47	-11.48	-15.78	-23.54
Saturation E	-8.6			
Saturation k_F (fm^{-1})	1.34			

TABLE VII. Partial wave contribution in MeV to the binding energy of nuclear matter for MDFP Δ2 [mesonic degrees of freedom potential with $\Delta(\pi\rho)$] at $k_F = 1.4$ fm^{-1}, with and without many-body effects. The same notation as in Table VI is used.

	MDFP Δ2	MDFP Δ2 No Δ effects Eq. (2.17)	MDFP Δ2 No mesonic effects Eq. (2.16)	MDFP Δ2 No many-body effects Eq. (2.18)
$^1S_0$	-13.48	-15.09	-16.28	-20.44
$^3P_0$	-3.72	-3.84	-3.89	-4.06
$^1P_1$	3.80	3.79	3.79	3.75
$^3P_1$	12.77	12.29	12.00	11.25
$^3S_1$	-19.09	-19.85	-22.10	-24.51
$^3D_1$	1.73	1.73	1.72	1.72
$^1D_2$	-2.59	-2.71	-2.76	-2.91
$^3D_2$	-4.51	-4.51	-4.54	-4.54
$^3P_2$	-6.40	-6.97	-7.30	-8.34
$^3F_2$	-0.62	-0.52	-0.50	-0.43
$J = 3$	3.21	3.19	3.15	3.13
$J = 4$	-1.78	-1.78	-1.79	-1.80
$5 \leqslant J \leqslant 12$	0.53	0.53	0.53	0.52
Total potential E	-30.15	-33.76	-37.98	-46.66
Kinetic E	24.02	24.02	24.02	24.02
E	-6.14	-9.74	-13.96	-22.64
Saturation E	-6.8			
Saturation k_F (fm^{-1})	1.25			

TABLE VIII. Partial wave contributions in MeV to the binding energy of nuclear matter for MDFP and MDFPE (mesonic degrees of freedom potentials without and with eikonal form factor, respectively) at $k_F = 1.4$ fm^{-1}, with and without many-body effects. The same notation as in Table VI is used except that "no mesonic effects" now refers to the use of Eq. (2.19) to define V_{eff}. The results for MDFP are taken from Ref. 6.

	MDFPE	MDFPE No mesonic effects Eq. (2.15)	MDFP	MDFP No mesonic effects Eq. (2.15)
$^1S_0$	-17.72	-18.45	-17.15	-17.56
$^3P_0$	-3.79	-3.83	-3.79	-3.80
$^1P_1$	4.30	4.29	3.31	3.33
$^3P_1$	11.17	11.10	11.34	11.25
$^3S_1$	-25.64	-27.00	-20.36	-22.36
$^3D_1$	1.49	1.48	1.38	1.38
$^1D_2$	-2.60	-2.61	-2.77	-2.77
$^3D_2$	-4.50	-4.51	-4.46	-4.48
$^3P_2$	-7.85	-7.95	-8.33	-8.45
$^3F_2$	-0.63	-0.63	-0.63	-0.63
$J = 3$	3.07	3.05	2.79	2.77
$J = 4$	-1.73	-1.73	-1.76	-1.76
$5 \leqslant J \leqslant 12$	0.51	0.51	0.49	0.48
Total potential E	-43.92	-46.28	-39.96	-42.60
Kinetic E	24.02	24.02	24.02	24.02
E	-19.90	-22.26	-15.93	-18.59
Saturation E	-27.6		-19.5	
Saturation k_F (fm^{-1})	1.87		1.75	

the propagator in these terms. The difference between the first and second columns of the tables should be a direct measure of the amount of intermediate range attraction replaced by the isobars and the results indicate this is somewhat larger for MDFPΔ2 than for MDFPΔ1.

In a similar way, the many-body effects from the mesonic degrees of freedom can be excluded by using Eq. (2.15) or (2.16) instead of Eq. (2.14) to define V_{eff}. These effects are repulsive again since self-consistent energies are used to evaluate the starting energy in the propagators of V_{OBE}, $V_{N\Delta}$, and $V_{\Delta\Delta}$. For MDFPE (see Table VIII) the resulting change in the binding energy is about 2.4 MeV vs 2.7 MeV for MDFP. Since MDFPE is more deeply bound, the difference between kinetic and self-consistent energies will be larger which would imply a larger effect for MDFPE. The fact that the opposite behavior is seen could be a result of the suppression of the terms second order in V_{eff} relative to the Born term for MDFPE as reflected in the D-state probability for the deuteron since as mentioned previously, these changes in the propagator are important only in second order terms.

For MDFPΔ1 and MDFPΔ2 the exclusion of many-body effects from MDF results in a change of about 7.8 and 7.3 MeV, respectively (see the third column of Tables VI and VII), which is much larger than in MDFPE. This is due to the fact that in the former cases there are two propagators for the isobar terms, one for each transition potential, which enhances the effect. Again, larger changes are seen when the ρ meson is included indicating more intermediate range attraction has been replaced by the isobars.

Finally, when no many-body effects of any kind are included by using Eq. (2.18) to define V_{eff}, the results in the last column are obtained. Here MDFPΔ1 is found to be more bound than MDFPΔ2 and this is partly due to different fits to the NN scattering data, particularly in the $J = 1$ P states. There is also an effect from the different values of M^* and A used. If the values used for MDFPΔ2 are also used in MDFPΔ1 then −23.96 MeV (instead of −23.54 MeV) is obtained. In addition, both these results lie well below that for MDFP. This is partially due to the fact that the former

were fitted to the *np* and the latter to the *pp* scattering length. Also, since the former are less bound, the propagator in the G matrix equation will be larger in magnitude yielding more binding energy.

IV. CONCLUSIONS

In this work, a study has been made in the nuclear many-body system of the effects of mesonic and isobar degrees of freedom (MDF and IDF) and the effects of the eikonal form factor in the meson-nucleon vertex. The results can be summarized as follows: First, the MDF play a singificant role in the many-body system. In ^{16}O, the consideration of these degrees of freedom yields a large increase in the radius, to a value near the experimental results. However, there is only a small decrease in binding energy, leading to different saturation properties for potentials including MDF than obtained from phase shift equivalent static potentials. This is due to the additional density dependence that is introduced through the starting energy dependence of the potential and leads to a different self-consistent wave function. These effects persist when the BHF equations are solved directly, avoiding the local density approximation.

The second main result observed in this work concerns the simultaneous inclusion of MDF and IDF. In ^{16}O, the addition of the latter yields additional repulsion. This is accompanied by an increase in the radius as would be expected for phase shift equivalent potentials with MDF. The main effect of the ρ meson is to replace part of the pionic form factor in the transition potentials. The results in ^{16}O are approximately the same using the π and ρ mesons in the transition potentials rather than using π mesons alone with a different cutoff in the form factor. The results obtained in nuclear matter are similar to those in ^{16}O.

Finally, when the dipole type form factors for the meson-nucleon vertices are replaced by eikonal form factors, the binding energy in ^{16}O increases. When MDF are considered for potentials with the eikonal form factor, the same effects can be seen as discussed above regarding this additional degree of freedom. However, the increase in radius is now smaller than above because the density dependence from the MDF is less important for this larger binding energy. In nuclear matter, the attraction is also increased, but this is just a reflection of the smaller D-state probability of the deuteron for this potential.

From these results it is clear that modifications of the *NN* interaction due to the nuclear medium play a decisive role, even in light nuclei. Thus, an understanding even of such gross features as binding energies and radii seems to require a very detailed model of the interaction. It would be interesting to see the effects when all fourth-order terms, e.g., crossed-box diagrams, in the interaction have been included.

---

*Also: Institut für Theoretische Kernphysik der Universität Bonn, D-5300 Bonn, West Germany.
†On leave of absence at the Physics Department, SUNY at Stony Brook, Stony Brook, New York 11794.

[1]G. E. Brown and A. D. Jackson, *The Nucleon-Nucleon Interaction* (North-Holland, Amsterdam, 1976).
[2]M. Bolsterli, Ann. Phys. (N.Y.) 62, 569 (1971).
[3]C. B. Dover and R. H. Lemmer, Phys. Rev. 165, 1105 (1968); 183, 908 (1969); J. Catara, M. Consoli, A. Insolia, L. Pappalardo, and S. Pappalardo, Nucl. Phys. A276, 433 (1977).
[4]W. D. Brown, R. D. Puff, and L. Wilets, Phys. Rev. C 2, 331 (1970).
[5]D. Schütte, Nucl. Phys. A221, 450 (1974).
[6]K. Kotthoff, R. Machleidt, and D. Schütte, Nucl. Phys. A264, 484 (1976).
[7]A. Faessler, H. Müther, R. Machleidt, and D. Schütte, Nucl. Phys. A262, 389 (1976).
[8]A. M. Green and J. A. Niskanen, Nucl. Phys. A249, 493 (1975).
[9]K. Holinde and R. Machleidt, Nucl. Phys. A280, 429 (1977).
[10]K. Holinde, R. Machleidt, A. Faessler, and H. Müther, Phys. Rev. C 15, 1932 (1977).
[11]B. D. Day and J. Coester, Phys. Rev. C 13, 1720 (1976).
[12]R. M. Woloshyn and A. D. Jackson, Nucl. Phys. A185, 131 (1972).
[13]K. Holinde and R. Machleidt, Nucl. Phys. A256, 479 (1976).
[14]K. Holinde and R. Machledit, Nucl. Phys. A256, 497 (1976).
[15]K. Kotthoff, K. Holinde, R. Machleidt, and D. Schütte, Nucl. Phys. A242, 429 (1975).
[16]K. Erkelenz, Phys. Rep. 13, 191 (1974).
[17]H. MacGregor, R. Arndt, and R. Wright, Phys. Rev. 182, 1714 (1969).
[18]K. Holinde, R. Machleidt, M. R. Anastasio, A. Faessler, and H. Müther, this issue, Phys. Rev. C 18, 870 (1978).
[19]H. A. Bethe, B. H. Brandow, and A. G. Petscheck, Phys. Rev. 129, 225 (1963).
[20]R. Machleidt, H. Müther, and A. Faessler, Nucl. Phys. A241, 18 (1975).
[21]P. U. Sauer, Nucl. Phys. A150, 467 (1970).
[22]R. J. Eden and V. J. Emery, Proc. R. Soc. London A248, 266 (1958).
[23]R. K. Tripathi, A. Faessler, and H. Müther, Phys. Rev. C 10, 2080 (1974).

[24]H. Müther, A. Faessler, and R. K. Tripathi, Nucl. Phys. A255, 132 (1975).
[25]L. D. Landau, Zh. Eksp. Teor. Fiz. 35, 95 (1958) [Sov. Phys.-JETP 8, 70 (1959)], and references therein.
[26]K. Holinde, K. Erkelenz, and R. Alzetta, Nucl. Phys. A194, 161 (1972); A198, 598 (1972).
[27]J. G. Zabolitzky, Phys. Lett. 47B, 487 (1973).